Electronic Rearrangement Induced by Substrate Analog Binding to the Enoyl-CoA Hydratase Active Site: Evidence for Substrate Activation†

Robert L. D'Ordine

Department of Chemistry, Brown University, Providence, Rhode Island 02912

Peter J. Tonge‡ and Paul R. Carey

National Research Council of Canada, Institute for Biological Sciences, Ottawa, Canada K1A OR6

Vernon E. Anderson*

Department of Biochemistry, Case Western Reserve University, 10900 Euclid Avenue, Cleveland, Ohio 44106

Received April 18, 1994; Revised Manuscript Received July 13, 1994®

ABSTRACT: A series of α,β unsaturated CoA thiol esters have been characterized spectroscopically when they form noncovalent complexes at the active site of enoyl-CoA hydratase. The UV spectra of all of the thiol esters display significant red shifts when the esters are bound to the crotonase active site. The red shift increases with the ability of a *para* substituent of substituted cinnamoyl-CoA thiol esters to donate electrons by resonance. The affinity of the substituted cinnamoyl-CoA thiol esters is enhanced by electron-donating substituents, with the slope of the log of the ratio of the inhibition constants versus σ_p^+ being near unity. Affinity is also increased by either *para* or *meta* electron-withdrawing substituents, suggesting that the enzyme stabilizes a partial positive charge at C-3. Binding to crotonase was shown to decrease the shielding of [3-^{13}C,3-^{2}H]cinnamoyl-CoA by +3.2 ppm, consistent with an increased partial positive charge at C-3. The Raman spectra of cinnamoyl-CoA bound at the crotonase active site similarly reflect the significant electronic ground state changes in the π electronic structure of the bound substrate. These data show that a major rearrangement of electrons occurs in the acryloyl portion of the cinnamoyl group upon binding, while only a minor perturbation occurs to the distribution of electrons in the phenyl ring. The strong electron polarization seen localized in the acryloyl moiety is consistent with a model in which the active site provides an electrophile at the C=O oxygen (e.g., in the form of a positive charge or strong H-bonds) and a nucleophile near the C-3 carbon of the cinnamoyl moiety.

Enoyl-CoA hydratase (crotonase,[1] EC 4.2.1.17) catalyzes the *syn* addition of water across α,β unsaturated CoA thiol esters (Willadsen & Eggerer, 1975). On the basis of thorough isotope effect studies (Bahnson & Anderson, 1989, 1991), it was proposed that crotonase catalyzes a concerted reaction where both the C—H and C—O bonds are formed in a single transition state, as shown in Scheme 1. An unactivated water molecule is shown as the nucleophile in this mechanism because there is a negligible solvent isotope effect. This would require an activated Michael acceptor, suggesting the possibility that the crotonase active site would induce a polarization of the double bond between C-2 and C-3 of the substrate. This paper presents unequivocal evidence that the active site of crotonase dramatically polarizes the π electrons of α,β unsaturated CoA thiol esters, thus enhancing the electrophilicity of the β carbon.

Changes in UV spectra by themselves are equivocal because they are determined by the energy difference between the ground and first excited electronic states. By quantifying and correlating the changes in affinity of a series of substituted cinnamoyl-CoA's and by examining the ^{13}C NMR and Raman spectra of bound cinnamoyl-CoA (Cin-CoA), we establish that the dramatic UV spectral shifts observed are related to changes in the ground state electron distribution in the conjugated thiol esters.

The cinnamoyl-CoA species used in this study are best viewed as thermodynamically stabilized substrates for the hydration reaction catalyzed by the enoyl-CoA hydratase. Recently, Mao et al. demonstrated that enoyl-CoA hydratase specifically catalyzed the dehydration of (*R*)-3-hydroxy-3-phenylpropanoyl-CoA to *trans*-cinnamoyl-CoA, with rates approaching those observed for the dehydration of 3-hydroxybutyryl-CoA (Mao et al., 1994). The equilibrium constant, however, greatly favors the dehydrated product. In our studies, we detected no decrease in the UV absorption over a period of days that could be attributed to the hydration of these thiol esters. That this nonreactivity is due to stabilization of the enoyl system by conjugation with additional π electrons is demonstrated by the effect on the equilibrium constant for hydration of 2,4-decadienoyl-CoA, where the additional double bond reduces the equilibrium constant for hydration by at least 1000-fold to ca. 0.003. Nevertheless, crotonase-catalyzed hydration can be detected by coupling the reaction to dehydrogenation of the product, 3-hydroxy-

† This work was supported by NIH Grant GM36562 (V.E.A.).

‡ Present address: The Picower Institute, 350 Community Drive, Manhasset, NY 11030.

® Abstract published in *Advance ACS Abstracts,* September 15, 1994.

[1] Abbreviations: CoA, coenzyme A; 3-CC-CoA, 3-chlorocinnamoyl-CoA; 4-CC-CoA, 4-chlorocinnamoyl-CoA; Cin-CoA, cinnamoyl-CoA; Cr-CoA, crotonyl-CoA; DAC-CoA, 4-(*N*,*N*-dimethylamino)cinnamoyl-CoA; DTNB, 5,5′-dithiobis(2-nitrobenzoic acid); crotonase, enoyl-CoA hydratase; 3-FC-CoA, 3-fluorocinnamoyl-CoA; HD-CoA, *trans,trans*-2,4-hexadienoyl-CoA; HPLC, high-performance liquid chromatography; MOXC-CoA, 4-methoxycinnamoyl-CoA; MC-CoA, 4-methylcinnamoyl-CoA; NOC-CoA, 4-nitrocinnamoyl-CoA; NMR, nuclear magnetic resonance; UV–vis, ultraviolet–visible; Quin2, 8-amino-2-[(2-amino-5-methylphenoxy)methyl]-6-methoxyquinoline-*N*,*N*,*N*′,*N*′-tetraacetic acid.

0006-2960/94/0433-12635$04.50/0

Scheme 1

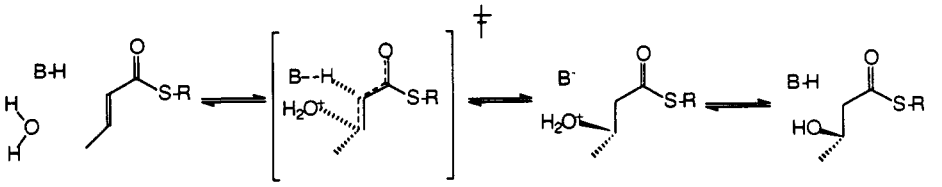

4-decenoyl-CoA (Yang et al., 1986). By analogy, the cinnamoyl-CoA–crotonase complexes that are spectroscopically characterized in this study are thermodynamically stabilized substrate complexes, which presumably are hydrated in vivo as demonstrated in the classic studies on the metabolism of ω-phenylcarboxylic acids by Knoop (1905).

MATERIALS AND METHODS

Chemicals. Coenzyme A (CoA) lithium salt was purchased from Sigma Chemical Co. [1-^{13}C,1-^{2}H]Benzaldehyde was from Isotec, Inc., triethyl phosphono[1-^{13}C]acetate was from Aldrich. Deuterium oxide (99.9%) was from Cambridge Isotope Labs. All substituted cinnamic acids were purchased from their respective sources in the *all-trans* or mostly *trans* forms. 4-(*N*,*N*-Dimethylamino)cinnamic acid, 4-methylcinnamic acid, 4-methoxycinnamic acid, 4-chlorocinnamic acid, 4-nitrocinnamic acid, 3-chlorocinnamic acid, 3-fluorocinnamic acid, *trans,trans*-2,4-hexadienoic acid, cinnamic acid imidazole, 1,1′-carbonyldiimidazole, *p*-nitrophenol, *N*,*N*-dicyclohexylcarbodiimide, 4-pyrrolidinopyridine, and triethyl phosphonoacetate were purchased from Aldrich or Sigma. All other chemicals were of reagent grade or better and used without further purification.

Synthesis of Coenzyme A Thiol Esters. 4-(*N*,*N*-Dimethylamino)cinnamoyl-CoA (DAC-CoA), 4-chlorocinnamoyl-CoA (4-CC-CoA), 4-methylcinnamoyl-CoA (MC-CoA), 4-methoxycinnamoyl-CoA (MOXC-CoA), 3-chlorocinnamoyl-CoA (3-chloro-CoA), 3-fluorocinnamoyl-CoA (3-FC-CoA), and *trans,trans*-2,4-hexadienoyl-CoA (HD-CoA) were synthesized by formation of the acylimidazole from their respective acids following the method of Kawaguchi (1981). 4-Nitrocinnamoyl-CoA (NOC-CoA) was synthesized by formation of the *p*-nitrophenyl ester through the use of *N*,*N*-dicyclohexylcarbodiimide and a 4-pyrrolidinopyridine catalyst following the procedure of Hassner (Hassner & Alexanian, 1978). The resulting *p*-nitrophenyl ester was then reacted in a fashion similar to that of the acylimidazoles to give the substituted cinnamoyl-CoA thiol ester. Cin-CoA was synthesized directly frim the acylimidazole available from Sigma.

[3-^{13}C,3-^{2}H]Cin-CoA was synthesized starting with [1-^{13}C,1-^{2}H]benzaldehyde and triethyl phosphonoacetate, using conditions similar to those of Meyers (1985). The resulting ethyl ester was then taken and hydrolyzed in ethanol/H_2O with 5 equiv of KOH at 65 °C until no ester was observed by TLC. TLC was performed using silica gel and a solvent system of 90% hexanes/10% ethyl acetate. Spots were visualized with I_2. The extracted acid was then subjected to the acylimidazole procedure described in the preceding paragraph.

[1-^{13}C]Cin-CoA was synthesized using the same procedures and conditions as were used for the [3-^{13}C,3-^{2}H]Cin-CoA derivative, except that triethyl phosphono[1-^{13}C]acetate was used as the source of the label.

The progress of all of the CoA acylation reactions was followed by testing for free thiol by assay with 1.0 mM 5,5′-dithiobis(2-nitrobenzoic acid) (DTNB) in 50 or 100 mM phosphate, pH 8.5 (Ellman, 1959). When no free thiol was observed, the resultant mixture was titrated to pH 4.5 with 1 M H_3PO_4, HCl, or acetic acid and extracted with 5 equal volumes of ethyl acetate to remove excess free acid. The cinnamoyl-CoA thiol ester was then purified by HPLC.

High-Performance Liquid Chromatography (HPLC). HPLC purifications of the cinnamoyl-CoA substrates were performed on an Alltech Econosil octadecylsilyl reverse phase column (10 mm × 250 mm) eluted with methanol, 1–10 mM phosphate (pH 4.5), and water at 3.0 mL/min. CoA thiol esters were detected by the ultraviolet absorbance of adenine at 260 nm.

Extinction Coefficients for the Cinnamoyl-CoA Thiol Esters. The extinction coefficients at 260 nm for most of the cinnamoyl-CoA thiol esters were reported previously (Person, 1981). These numbers were originally determined by the quantitation of thiol, produced by hydroxaminolysis, with DTNB (Ellman, 1959). We discovered, while trying to repeat these determinations, that this method is incompatible with the double bonds, under the reaction conditions, due to incomplete detection of the thiol from a competing Michael addition or due to incomplete hydrolysis of the thiol ester stabilized by conjugation. The extinction coefficients at 260 nm for the substituted cinnamoyl-CoA derivatives were determined by correlation of the cinnamoyl-CoA thiol ester concentration, by integration ratio, with an added internal standard of known concentration in the NMR spectrum. This concentration was then used to determine the extinction coefficient at 260 nm for each species by its absorbance in the UV. A weighed amount of potassium acetate in D_2O was used as the added internal concentration standard. The values reported are the average of two independent determinations that were always within 10% of each other. The method was checked for accuracy by testing butyryl-CoA, a CoA thiol ester with a known extinction coefficient. The value obtained was within 10% of the 15 400 M^{-1} cm^{-1} value determined by the DTNB hydrolysis method (Dawson et al., 1986). The values obtained are reported in Table 1.

Enzymes. Crotonase (enoyl-CoA hydratase, EC 4.2.1.17) was isolated using a procedure based on that of Steinman and Hill (1975) as modified by Bahnson (1990). The concentration of the crystalline crotonase was determined using the extinction coefficient of 27 800 M^{-1} cm^{-1} at 494 nm for the crotonase–DAC-CoA complex or by the extinction coefficient of 16 100 M^{-1} cm^{-1} at 280 nm for the crystalline protein (Hass & Hill, 1969).

NMR Spectroscopy. All ^{1}H NMR spectra were acquired on a Bruker AM 400 MHz NMR spectrometer in D_2O. The probe temperature was always 24–26 °C. Chemical shifts are reported with respect to external (trimethysilyl)propanesulfonic acid (DSS) or (trimethysilyl)propionic acid (TSP). The internal chemical shift standard was the triplet at 2.43 ppm due to protons (t, 2H) on C-6″ of the pantetheine backbone (Sarma & Lee, 1975).

The ^{13}C NMR spectra of [3-^{13}C,3-^{2}H]cinnamoyl-CoA were obtained using the same spectrometer as for ^{1}H at 100.61

MHz. All protein–protein substrate spectra were acquired in the ^{13}C–proton decoupled mode with a decoupler power of 0.5 W, a pulse width of 45 μs, and a recycle delay of 2.0 s. The protein–substrate spectra are the result of 20 000–26 000 transients each. Samples usually contained 2.0 mM crotonase active sites in 100 mM potassium phosphate, pD 7.8 ± 0.3 (70–90% D_2O), and varying amounts of Cin-CoA. Sample activity and pD were checked before and after experiments. Sample volumes were 400–500 μL in 5 mm quartz NMR tubes. The spectra of each crotonase and Cin-CoA sample were acquired prior to the addition of the substrate to the enzyme. Concentrated substrate stock solutions were used for addition to the crotonase samples to minimize dilution. An amount of substrate equal to approximately 0.75 of the crotonase concentration was added first, and then successive titrations were performed in order to observe both bound and free species. The experimental conditions used in these studies were adapted from those described by Jaffe and Markham (1987) for acquiring ^{13}C NMR spectra of labeled substrates when bound to large enzymes.

UV–vis Spectroscopy of Cinnamoyl-CoA's Complexed with Crotonase. All ultraviolet–visible experiments were carried out on a Hewlett-Packard 8452A diode array spectrophotometer with a quartz cell of 1 cm path length. Spectra were processed using the Hewlett-Packard diode array software. Crotonase stored as a crystalline solid was thawed and centrifuged. The precipitated crystals were resuspended in 50 mM potassium phosphate buffer at pH 7.01 and centrifuged once again to remove any denatured protein. The crotonase concentration was determined either by the extinction coefficient of 16 100 M^{-1} cm^{-1} at 280 nm (Hass & Hill, 1969) or by titration of the active sites with DAC-CoA and quantitation of the DAC-CoA–crotonase complex.

The spectrophotometer was blanked using the appropriate amount of 50 mM phosphate buffer before spectra of crotonase, crotonase and bound cinnamoyl-CoA, and free cinnamoyl-CoA were taken. The cinnamoyl-CoA–crotonase samples contained between 1 and 100 μM crotonase in a volume of 300–500 μL. Each sample was titrated to crotonase saturation, determined by the observation of saturation of the absorbance at the λ_{max} of the bound form. Crotonase showed saturation for all of the cinnamoyl-CoA derivatives tested in this manner. Difference spectra λ_{max} were obtained by subtraction of the crotonase spectrum and the free cinnamoyl-CoA spectrum from the crotonase–cinnamoyl-CoA-bound spectrum.

Spectra in Varying H_2SO_4 Solutions. Varying amounts of H_2SO_4 were used to change the solvent polarity and to protonate the thiol ester carbonyl. Spectra were obtained by first making a solution from 0–90% H_2SO_4 (v/v) in water and blanking the spectrophotometer. To each solution was added HD-CoA, MOXC-CoA, or Cin-CoA. The sample was mixed rapidly and a spectrum was recorded.

DAC-CoA–Crotonase Complex. The dissociation constant for the DAC-CoA–crotonase complex was found to be ca. 1 μM, while the λ_{max} is displaced by 90 nm. Consequently, DAC-CoA in excess of 20 μM will saturate the crotonase active sites while contributing minimally to the absorbance at 494 nm, allowing the concentration of crotonase active sites to be determined spectrophotometrically. This method obviates the need to use the extinction coefficient (16 100 M^{-1} cm^{-1}) at 280 nm, which is only useful for pure enzyme, or a more cumbersome kinetic quantitation of activity to determine crotonase concentrations. Using a solution of known DAC-CoA concentration and excess crotonase, ca. 1 μM amounts of DAC-CoA were added to the solution. Under these conditions, all of the DAC-CoA is bound and the ΔA_{494}/[DAC-CoA] ratio yields the extinction coefficient, ϵ_{494}, for the complex. This ratio is constant for several additions of DAC-CoA, proving that the crotonase was present in sufficient excess. The ϵ_{494} of 27 800 M^{-1} cm^{-1} was subsequently used to quantify crotonase active sites in the presence of excess DAC-CoA.

K_i's for the Cinnamoyl-CoA Substrates. The binding or inhibition equilibrium constants were found by monitoring the first-order approach to equilibrium with Cr-CoA (Fersht, 1985). Determinations were performed at 10 μM, $^1/_2K_m$ (Waterson & Hill, 1972), for Cr-CoA in 50 mM potassium phosphate, pH 7.0. Crotonase concentrations were in the nanomolar range, typically 1–2 nM. Inhibitor concentrations ranged from 0.5 to ca. 100 μM. Each of the experiments for a single determination, at a given concentration of inhibitor, was performed in duplicate. First-order fits of the loss of absorbance at 260 and/or 280 nm were plotted with time. The reciprocals of the first-order rate constants obtained were plotted versus inhibitor concentration to give a straight line based on the following equation for inhibition kinetics:

$$k_{obs} = \frac{k_{max}A}{1 + A/K_a + I/K_i} \quad (1)$$

where $k_{max} = k_0Et$, I is the inhibitor concentration, $K_a = K_m$ for crotonyl-CoA, A is the substrate concentration, and K_i is the inhibition constant for the cinnamoyl-CoA derivative in question. This equation can be algebraically transformed into the following equation for a straight line:

$$1/k_{obs} = C/k + (I/K_i)(1/k) \quad (2)$$

where $C = 1 + A/K_m$ and $k = k_{max}$. Plotting $1/k_{obs}$ versus I will give the straight line with a slope of $(1/K_i)(1/k)$ and an intercept of C/k, from which k can be found and in turn the K_i can be obtained since all other values are known.

Metal Ion Analysis. 8-Amino-2-[(2-amino-5-methylphenoxy)methyl]-6-methoxyquinoline-*N*,*N*,*N*′,*N*′-tetraacetic acid (Quin2), a Ca^{2+} and Zn^{2+} chelator (Tsien et al., 1982), was used as a probe for metal ions in crotonase. Quin2 has a characteristic UV–vis absorbance λ_{max} at 262 nm that is perturbed when it binds divalent metal ions. Ca^{2+} shifts the absorbance to 242 nm with equal intensity, and Zn^{2+} shifts the absorbance to 248 nm with diminished intensity. A sample of crystalline crotonase was centrifuged, and the crystals were washed carefully with distilled deionized H_2O and resuspended in 50 mM sodium phosphate (pH 7.0) in distilled deionized H_2O. The concentration of the crotonase was determined, and the sample was denatured by heating at 80 °C for 15–30 min. Solutions of Quin2 at 10 μM were titrated with the denatured crotonase solutions up to 60 μM concentration, and no perturbation of the 262 nm absorbance was observed. The same solutions were titrated with standard solutions of Ca^{2+} and Zn^{2+}, and it was found that Quin2 absorbance was perturbed by a <1 μM metal ion concentration.

Alternatively, crystalline crotonase was submitted to inductively coupled plasma mass spectrometric (ICP-MS) analysis for heavy metals, with specific attention paid to determining Ni, Zn, and Fe by selected ion monitoring. Crotonase was recrystallized by ethanol addition from a 1 mM solution of Tris–EDTA (pH 7.5) made from Tris base and the acid form of EDTA. For the metal analyses, samples of 1–2 mg were digested in concentrated nitric acid for 1 h

Table 1 [a]

trans-p-cinnamoyl-CoA derivative,[e] R =	ϵ_{260} (cm^{-1} M^{-1})	$A_{260}/A_{\lambda max}$[f]	λ_{max} (nm)[b]	λ_{max} bound (nm)[c]	shift (nm)	λ_{max} difference spectra (nm)[d]	difference spectra shift (nm)
4-dimethylamino	16 500	0.98	404	494	90	494	90
4-methoxy	20 100	1.1	334	375	41	380	46
4-methyl	16 400	0.96	318	341	30	359	41
H (cinnamoyl)	17 600	0.94	309	337	28	349	40
4-chloro	17 800	0.95	315	341	26	347	32
4-nitro	25 000	1.0	323	343	20	348	25

[a] Spectra were acquired as described in Materials and Methods. [b] Maximum (in nanometers) for the band due to the conjugated system of the substrate chromophore free in solution. [c] Maximum for the band due to the conjugated system of the substrate chromophore bound to the enzyme minus enzyme background. [d] Maximum for the band due to the conjugated system of the substrate chromophore minus the contribution due to free chromophore under the same conditions without enzyme. [e] Arranged in decreasing order of electron-donating capability. [f] For pure samples, as judged by NMR, these ratios were reproducible to ±0.1.

at 110 °C and subsequently dissolved in 7.5 mL of deionized distilled water containing a ^{45}Sc internal standard. Blank samples and samples containing 2.5 and 5.0 μg of Fe, Ni, and Zn were used to calibrate the quantitation. The samples were analyzed on a Perkin-Elmer ICP-MS.

Raman Spectroscopy of Cin-CoA. Acquisition of the spectra using a single monochromator equipped with a CCD detector and a supernotch filter (Kim et al., 1993) enabled data to be collected under normal Raman (i.e., nonresonance) conditions. Raman spectra were acquired using 450 mW of 488 nm radiation from an argon ion laser and 90° scattering geometry. Samples typically were 0.16 mL and contained 200 μM Cin-CoA and 225 μM crotonase active sites for acquisition of the bound spectra. More details are given in the legend to Figure 5.

RESULTS

Equilibrium Binding. All of the α,β unsaturated CoA thiol esters in this study had at least an additional conjugated double bond. Hydration of the α,β unsaturated double bond isolates the additional π system. Consequently, the equilibrium constant for hydration is reduced from 3.5 for Cr-CoA to less than 0.05 for all of the CoA thiol esters, with extended conjugation in these experiments. To test for possible hydration, ca. 50 μM CoA thiol ester solutions were incubated with purified crotonase. We saw no evidence for significant hydration of any of the derivatives by monitoring the change in UV absorbance as a function of time. It is possible to demonstrate hydration of decadienoyl-CoA by coupling the reaction to the dehydrogenation of the product with 3-hydroxyacyl-CoA dehydrogenase (Yang et al., 1986). This observation is in contrast to an earlier characterization of the reaction of substituted cinnamoyl-CoA's with crotonase (Person, 1981). These earlier reactions may have been due to a thiol esterase present in the isolated crotonase or due to excess thiol in the reaction buffer adding nonenzymatically to form a Michael adduct. The constancy of the absorbance at the λ_{max} of the conjugated system also suggests that the enzyme does not catalyze the *cis–trans* isomerization about the α,β unsaturation or that the equilibrium constant for this isomerization is too small for the *cis* isomer to be present at a significant concentration, as the *cis*-cinnamic acid has an extinction coefficient one-half that of the *trans* isomer (Eliel, 1962).

UV–vis Spectra. The cinnamoyl-CoA thiol esters exhibited significant UV–vis shifts on binding to crotonase. The spectra of free and bound DAC-CoA are shown in Figure 1. The wavelength changes observed for all of the cinnamoyl-CoA's are compiled in Table 1. All of the cinnamoyl-CoA's were inhibitors of Cr-CoA hydration, and the experimental inhibition constants are listed in Table 2. The data for all electron-donating *para* substituents were plotted as a linear free energy correlation, $\log K_x/K_h$ versus σ_p^+ (Lefler & Grunwald, 1963). The resultant line, with a slope of 0.75, is shown in Figure 2a. Electron-withdrawing substituents, both *para* and *meta*, also enhanced the affinity of the cinnamoyl-CoA for the crotonase active site. The correlation obtained with the *para* substituents with σ_p is shown in Figure 2b. The correlation is not as strong as that observed with the electron-donating species because the effects are smaller and more prone to be masked by competing effects, such as desolvation or more localized interaction between the substituent and the active site. Still, all of the cinnamoyl-CoA's substituted with electron-withdrawing groups have an equal or greater affinity for the enzyme than Cin-CoA.

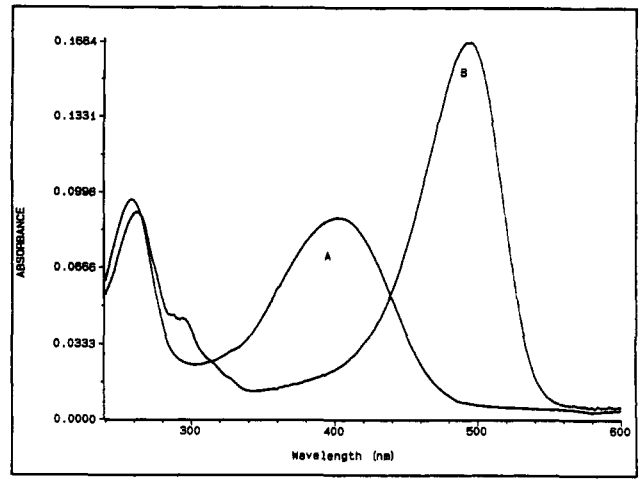

FIGURE 1: UV–vis spectra of 4-(*N*,*N*-dimethylamino)cinnamoyl-CoA: (A) 6 μM free DAC-CoA in 50 mM potassium phosphate (pH 7.0); (B) 6 μM DAC-CoA bound to excess crotonase (21 μM) under the same conditions as the free spectrum minus the contribution due to the enzyme absorbance spectrum (not shown).

Table 2

CoA derivative	σ_p^+ [a]	K_i (μM)[b]	K_x/K_h	$\log K_x/K_h$
4-dimethylamino	−1.7	1.8	0.049	−1.31
4-methoxy	−0.78	8.0	0.22	−0.67
4-methyl	−0.31	17	0.46	−0.33
H (cinnamoyl)	0	37	1	0
4-chloro	0.11	16	0.36	0.44
4-nitro	0.79	3.7	0.14	0.84
CoA derivative	**σ_m**	**K_i (μM)**	**K_x/K_h**	**$\log K_x/K_h$**
3-chloro	0.34	30	0.82	−0.088
3-fluoro	0.37	40	1.08	0.034

[a] All σ_p^+ and σ_p constants are from Lefler and Grunwald (1963). [b] Average of two or more duplicate measurements. σ_p values for 4-chloro- and 4-nitro-CoA are 0.23 and 0.78, respectively.

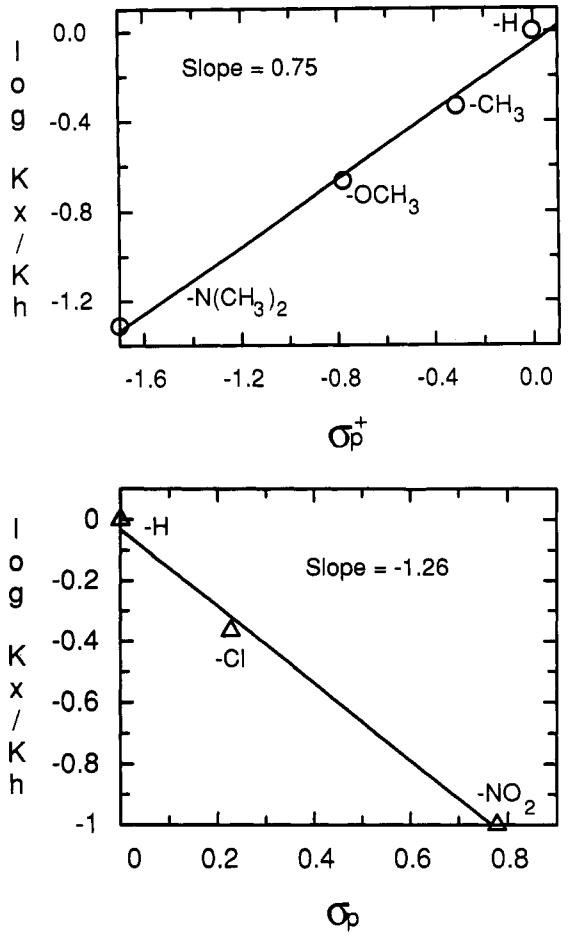

FIGURE 2: Linear free energy correlations. (A, top) Plot of the log of the ratio of the binding affinities of electron-donating *para*-substituted cinnamoyl-CoA's to Cin-CoA versus the corresponding σ_p^+ values. Results of the linear fit: slope, 0.754; intercept, –0.0521; and $r = 0.997$. (B, bottom) Plot of the log of the ratio of the binding affinities of electron-withdrawing *para*-substituted cinnamoyl-CoA's versus the corresponding σ_p values. Results of linear fit: slope, –1.26; intercept, –0.0323, and $r = 0.997$. K_x is the corresponding inhibition constant, K_i, for the crotonase-catalyzed hydration of crotonyl-CoA for each of the substituted species. K_h is K_i for Cin-CoA.

The large UV–vis red shift observed with the DAC-CoA–crotonase complex is similar to that observed when 4-(*N*,*N*-dimethylamino)cinnamaldehyde complexes with the active site Zn^{2+} of alcohol dehydrogenase (Dahl & Dunn, 1984) and aldehyde dehydrogenase (Dunn & Buckley, 1985). To determine whether a previously undetected active site metal was responsible for the observed shift, 60 μM crotonase was heat denatured, and the resultant solutions were analyzed by Quin2 for metal ions as described in the Materials and Methods section. A change in the absorbance of Quin2 is diagnostic for divalent cation complexation. No absorption change was observed. However, as a positive control, the addition of 1 μM Zn^{2+} or Ca^{2+} generated a detectable difference, indicating that stoichiometric equivalents of these metals are not present in the crystalline crotonase.

The effects of varying concentrations of H_2SO_4 on the UV spectrum of MOXC-CoA are shown in Figure 3. The spectral variation is consistent with high concentrations of H_2SO_4 protonating the conjugated thiol ester and generating a new species with a λ_{max} that is red shifted by 90 nm. The site of protonation is presumably the thiol ester carbonyl since the H_o of ca. –7 is expected for a carbonyl, and similar spectral changes were observed with Cin-CoA and HD-CoA. At lower H_2SO_4 concentrations, there is a very small red shift, <10 nm, as the polarity and H-bond-donating strength of the solvent both increase.

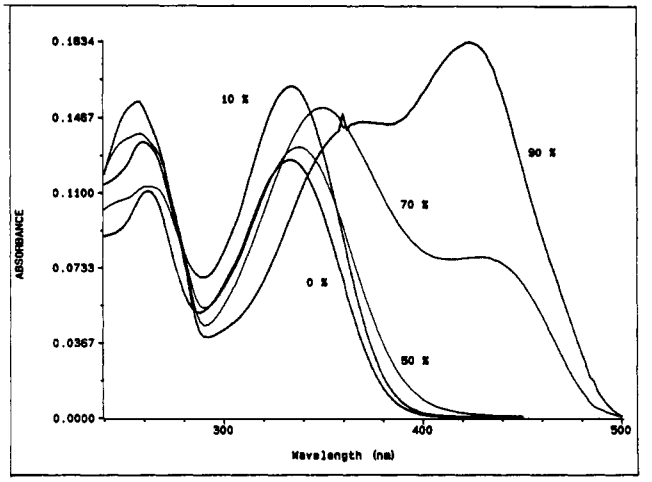

FIGURE 3: UV–vis spectra of MOXC-CoA in increasing concentrations of H_2SO_4. The volume percent H_2SO_4 for each spectrum is noted. The spectra clearly show two species in the presence of 50% H_2SO_4. The second species present at high percent H_2SO_4 is red shifted 90 nm, presumably by protonating the carbonyl.

^{13}C NMR. The ^{13}C NMR spectrum of [3-^{13}C,3-^{2}H]Cin-CoA shown in Figure 4 also corroborates the change in electron distribution on binding of the unsaturated CoA thiol ester to the crotonase active site. The free [3-^{13}C,3-^{2}H]Cin-CoA has a resonance at 144.0 ppm that is shifted to 147.2 ppm on binding to the active site. This 3.2 ppm increase in the ^{13}C chemical shift is most simply interpreted as a decrease in π electron density at the β carbon, leading to the observed deshielding. Controls showed that the bound species was noncovalent, since it could be washed out of the active site by titration with excess unlabeled material.

Raman Spectra. As a result of the high light-collecting efficiency of the Raman spectrometer and the polarizable nature of the cinnamoyl group (giving rise to high Raman intensities), it was possible to obtain high-quality data at concentrations of 100–200 μM under normal, i.e., nonresonance, Raman conditions. The Raman spectra seen in Figures 5 and 6, for the unlabeled and [1-^{13}C]Cin-CoA, respectively, are dominated by intense features in the double bond region, 1500–1700 cm^{-1}, and the present discussion will focus on this region. Spectral interpretation is based on the data in Figures 5 and 6, literature assignments, and a wealth of data to be published separately. It is governed by the following considerations. The first observation is that pure carbonyl stretching bands are weak and broad and cannot be identified in Figures 5 and 6; however, they can be observed in the IR at higher frequency for the unbound species.[2] Secondly, there are two intense bands near 1600 and 1625 cm^{-1} that are due to the normal modes of the phenyl ring. The modes are designated 8a and 8b and have been discussed extensively in the literature (Varsanyi, 1969; Harada & Takeuchi, 1986, Austin et al., 1992). Finally, a third intense feature is associated with a stretching motion of the acryloyl moiety C=C—C(=O), and its exact composition depends on the electron density distribution in that group. However, C=C and C=O stretches usually make important contributions. These three intense bands are most easily identified in the spectra of the ^{13}C derivative (Figure 6): the phenyl modes are seen near 1625 and 1599 cm^{-1}, and the acryloyl stretch is seen

[2] Peter Tonge and Paul Carey, unpublished observations.

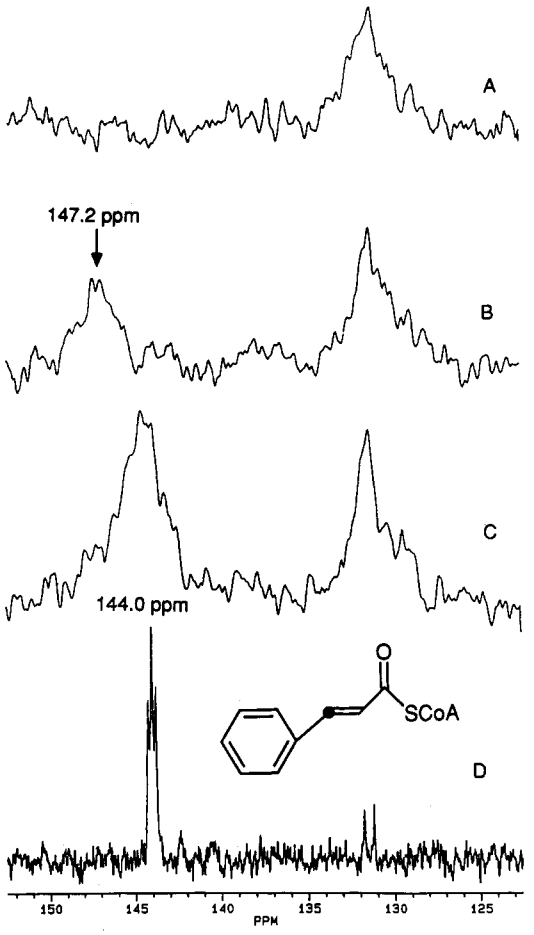

FIGURE 4: 100.6 MHz ^{13}C NMR spectra of crotonase and [3-^{13}C,3-^{2}H]Cin-CoA. (A) Spectrum of 2.0 mM crotonase showing the aromatic-unsaturated region of the protein. (B) Spectrum of [3-^{13}C,3-^{2}H]Cin-CoA bound to crotonase. Cin-CoA/crotonase = 0.8. The resonance at 147.2 ppm is due to bound [3-^{13}C,3-^{2}H]Cin-CoA. (C) Spectrum of [3-^{13}C,3-^{2}H]Cin-CoA bound to crotonase. Cin-CoA/Crotonase = 1.5. Note the averaging effect due to fast (on the NMR time scale) exchange between free and bound species as increasing the concentration of [3-^{13}C,3-^{2}H]Cin-CoA causes the signal to shift toward free and to broaden. (D) Spectrum of 3 mM [3-^{13}C,3-^{2}H]-Cin-CoA. The signal at 131.5 ppm is due to an unknown impurity that is not observed in either the UV or ^{1}H NMR of the sample. All spectra with crotonase present were processed with 25 Hz line broadening and are the result of 20–26 000 transients. The spectrum of [3-^{13}C,3-^{2}H]Cin-CoA was processed using 5 Hz line broadening and only 640 transients were acquired. All other conditions were as described in Materials and Methods. The dot on C-3 of Cin-CoA marks the site of isotopic substitution.

at 1529 cm^{-1} (bound form) and as a shoulder near 1580 cm^{-1} (free form).

The spectrum of unbound, unlabeled Cin-CoA (Figure 5) is complicated by the fact that the acryloyl mode lies in the same wavenumber region as the phenyl ring modes and probably undergoes strong vibrational mixing with them. Thus, the two ring modes and single acryloyl mode cannot be identified by inspection. However, for the bound ^{12}C form, the large shift to lower frequency undergone by the acryloyl mode displaces it from the ring vibrations, and the three individual bands can again be seen. In general, the large changes seen in the double bond region upon binding are evidence that a major electronic redistribution is occurring in the conjugated π system when the ligand binds to crotonase.

Metal Analyses. Neither the fluorescence studies with Quin2 or the ICP-MS detected the presence of a significant concentration of heavy metal ions. The ICP-MS provided limits of <0.05 equiv of Ni, Zn, or Fe present in the active

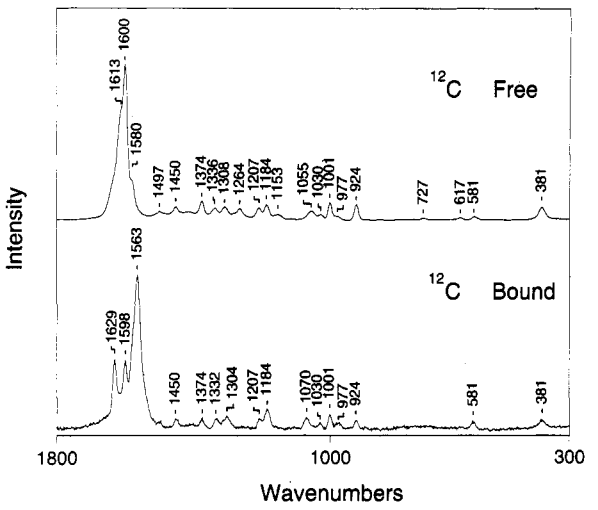

FIGURE 5: Raman spectra of unlabeled Cin-CoA free in solution and bound to crotonase obtained using 450 mW, 488 nm laser excitation and spectral resolution of 8 cm^{-1}. (A) 0.5 mM Cin-CoA in 20 mM phosphate (KH_2P) buffer (pH 7.4) containing 3 mM EDTA and 0.2 M KCl. 10 scans each with 10 s exposure time were acquired and coadded. Subsequently a buffer spectrum, acquired under identical conditions, was subtracted. (B) Cin-CoA bound to crotonase. Initially a Raman spectrum of 0.16 mL of 0.225 M crotonase in 20 mM phosphate (KH_2P) buffer (pH 7.4) containing 3 mM EDTA and 0.2 M KCl was obtained with 10 s × 10 scans. Subsequently 1.1 μL of 30 mM Cin-CoA was added and the spectral acquisition repeated. The difference Raman spectrum of bound Cin-CoA was obtained by subtraction.

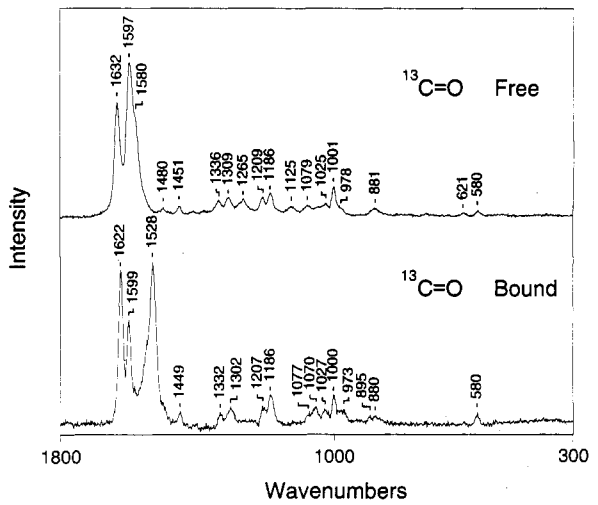

FIGURE 6: Raman spectra of ^{13}C=O Cin-CoA free in solution and bound to crotonase. Conditions and data acquisition parameters were identical to those described in the legend to Figure 5: (A) ^{13}C=O Cin-CoA in phosphate buffer; (B) ^{13}C=O Cin-CoA bound to crotonase.

crotonase crystals and minimal amounts of Mg, Mn, or Ca, whose catalytic requirements were detected by scanning. The constant catalytic activity in the presence of excess EDTA minimizes the potential that any of these ions are catalytically essential.

DISCUSSION

The large spectral shifts observed in the UV spectra when the conjugated CoA thiol esters bind to the crotonase active site are strong evidence that the electronic environment of the active site is different from that of the solvent. The molecular interpretation of such UV spectral shifts can be ambiguous because the observed red shifts can be due to either a decrease in the energy of the electronic excited state or a relative increase

Scheme 2

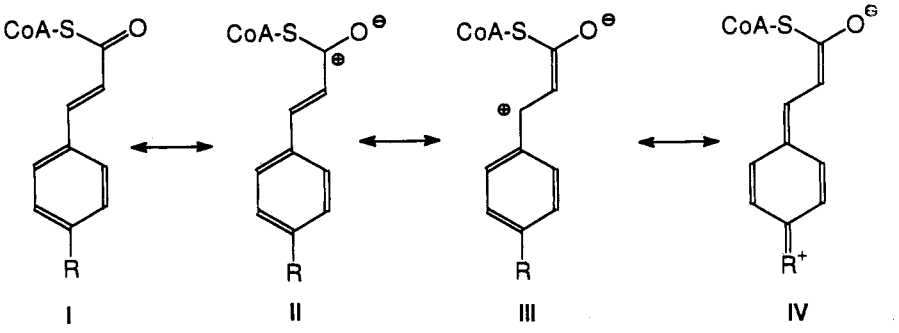

in the energy of the ground state. If the major source of the red shift is a stabilization of the electronic excited state, the relevance to the enzyme's catalytic mechanism is questionable. The accompanying changes in both the Raman and ^{13}C NMR spectra of the bound Cin-CoA indicate that there are significant changes in the ground state that must give rise to at least part of the changes seen in the UV spectrum.

The increasing red shift with increased electron-donating potential of the *para* substituent shown in Table 1 is anticipated for polarization of the α,β unsaturated species, in a fashion that would enhance the ability of Cr-CoA to function as a Michael acceptor. To test whether this graded red shift arises from complete protonation of the carbonyl, as once proposed for the UV shift in keto steroid isomerase (Kuliopoulos et al., 1989), or from H-bonding to the carbonyl, as suggested by Gerlt and Gassman (Gerlt & Gassman, 1992; Gerlt et al., 1991), the spectra of HD-CoA, Cin-CoA, and MOXC-CoA were acquired in varying concentrations of H_2SO_4 (see Figure 3). There are two important features of the spectra of all three compounds in H_2SO_4: (a) protonation of any α,β unsaturated CoA thiol ester generates a 90 nm red shift and (b) the extremely strong H-bond solvent of 30–50% H_2SO_4 only generates at most a 10–15 nm red shift. Overall, the experimental results cannot be accommodated by an explanation based solely on protonating or H-bonding the carbonyl of the thiol ester. The observed red shifts for the *para*-substituted cinnamoyl-CoA's of 25–46 nm, increasing with increased polarizability, cannot be explained by an equilibrium mixture of protonated and unprotonated species at the active site being biased more and more toward the protonated species, because this would predict a spectrum with two maxima whose relative intensities varied as observed in the titration in Figure 3. Secondly, the shift observed with MOXC-CoA is far greater than that generated by 50% H_2SO_4, suggesting that the simple explanation of stronger H-bonds to the carbonyl is inadequate to explain the large spectral shifts observed. The Raman data, discussed in the following, support the conclusions that protonation of the carbonyl oxygen is not occurring and that a mixture of protonated and unprotonated bound ligands does not exist.

The ease of polarizing the conjugated π system and the affinity of the substituted cinnamoyl-CoA's was demonstrated by the linear correlation of log K_x/K_h with σ_p^+. The slope, ρ^+, obtained is 0.75. The σ_p^+ constants provide a positive log–linear relationship when the reaction generates an electron deficient center stabilized by resonance electron donation from the *para* substituent. The magnitude of the slope indicates that the extra stabilization by resonance is 75% of the stabilization of the transition state in the defining reaction; the solvolysis of *tert*-cumyl chloride (Brown & Okamoto, 1958). This solvolysis is an S_N1 reaction where a large partial positive charge on the benzylic carbon is anticipated in the transition state. In the cinnamoyl-CoA series, the resonance stabilization of an increased positive charge may occur at either the β or carbonyl carbons (or more realistically both), as shown in the resonance structures II and III of Scheme 2.

Scheme 3

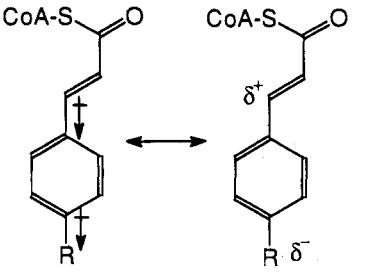

Surprisingly, the electron-withdrawing substituents also enhanced the affinity of the substituted cinnamoyl-CoA's for the active site, as shown in Figure 2b. The UV–vis spectra did not predict this enhanced affinity because the red shift decreases continuously from Cin-CoA through the halogen-substituted cinnamoyl-CoA's to NOC-CoA. The hydrophobic *p*-Cl and hydrophilic *p*-NO_2 substitutions both produce enhanced affinity, making it difficult to ascribe the enhanced affinity to the polarity of the binding site. The *meta*-substituted 3-CC-CoA also has an enhanced affinity, indicating the potential for this being an inductive effect with the enzyme having an greater affinity for α,β unsaturated thiol esters with an increased positive charge at the β carbon (i.e., C-3) and without any increased electron density on the carbonyl oxygen, as shown in Scheme 3. Taken together, these two effects indicate that the enhanced affinity of the substituted cinnamoyl-CoA's is due to *both* an increased polarization of the carbonyl and an increased partial positive charge on the β carbon.

This suggestion was pursued by an attempt to directly observe an increased partial positive charge at the β carbon with ^{13}C NMR. Due to the tumbling correlation and relaxation times associated with large proteins (Allerhand, 1979), and consequently with ligands bound to these enzymes, the ^{13}C NMR line width of substrate bound in the active site of crotonase, a homohexamer of ca. 168 000 M_r, is anticipated to be very broad. [3-^{13}C,3-^{2}H]Cin-CoA was synthesized with the ^{2}H present on the labeled carbon to minimize the ^{13}C–^{1}H dipolar relaxation, the dominant contributor to relaxation at these molecular weights and tumbling correlation times, thus minimizing the anticipated line width.

While the observed increase in chemical shift of +3.2 ppm observed in Figure 4 could be attributed to other factors, such as anisotropic field effects from aromatic active site residues, the UV spectral changes, the strong Hammett correlation, and the Raman spectra all point to the most probable cause being the redistribution of π electrons. The magnitude of the chemical shift can be correlated with an absolute decrease of 0.02e by the Spiesecke–Schneider relationship of 160 ppm downfield shift per π electron (Spiesecke & Schneider, 1961). This value presumably is less than that which would be observed for Cr-CoA, where there is no potential for the partial positive charge to be diminished by resonance with the phenyl ring.

The 3.2 ppm downfield chemical shift could correspond to a dramatic increase in chemical reactivity. In an NMR study of [*nicotinamide*-4-^{13}C]NAD$^+$ bound to UDP-galactose 4-epimerase, a similar 2.77 ppm downfield shift was observed (Burke & Frey, 1993). The C-4 position of NAD$^+$ is similar to the C-3 of Cin-CoA in that they are both sp^2 hybridized and conjugated to other π bonds. Burke and Frey (1993) demonstrated there was a linear correlation between the 4-^{13}C chemical shift and the log of the rate constant for $NaCNBH_4$ reduction at C-4 of a series of *N*-alkyl-substituted nicotinamides. The slope of between 1.03 and 1.23, depending on conditions, demonstrates that a 3 ppm chemical shift could easily correspond to an enhanced electrophilicity of over 3 orders of magnitude.

The Raman data for Cin-CoA provide additional strong evidence that large scale rearrangement of the π electrons occurs upon binding. However, this effect seems to be localized in the acryloyl portion of the cinnamoyl moiety, with only minor perturbations occurring in the phenyl ring. Using the assignments made in the Results section, the ring modes 8a and 8b only undergo modest shifts for the ^{13}C derivative upon binding, from 1632 and 1597 to 1622 cm^{-1} and 1599 cm^{-1}. These modes also appear at similar positions in the bound ^{12}C compound, viz., at 1629 and 1598 cm^{-1}. However, the acryloyl mode undergoes a large shift to lower frequencies upon binding, from ca. 1600 to 1563 cm^{-1} for the ^{12}C analog and from ca. 1580 to 1529 cm^{-1} for the ^{13}C compound, i.e., a shift of 40–50 cm^{-1}.

Three conclusions follow from these observations. Firstly, the cinnamoyl's phenyl ring retains its benzenoid character on the enzyme. This eliminates the possibility that the ring assumes a quinonoid-like structure upon binding, since the ring modes 8a and 8b are absent from the Raman spectra of quinone structures.[2] Secondly, in a related manner, the Raman data are inconsistent with protonation of the acryloyl C=O oxygen on the enzyme, since the prevalence of resonance structures analogous to IV with the O protonated would be expected to have a major effect on ring modes 8a and 8b. Thirdly, the large redistribution of π electrons seems to be mainly limited to the acryloyl moiety. In all likelihood, the acryloyl mode is a delocalized vibration involving the motion of many of that group's atoms and is mainly stretching in character, since an in-phase stretch on the acryloyl's long axis will give rise to large changes in polarizability and the observed large relative intensity of this mode seen in Figures 5 and 6.

The challenge now lies in producing a model that explains all of the spectroscopic results. The large changes in ground state electron distribution evidenced by the ^{13}C NMR and Raman data appear to be fairly localized in the acryloyl portion of the bound molecule. This and the magnitude of the changes observed are difficult to explain simply in terms of enhanced hydrogen bonding to the carbonyl oxygen in the binding site.

Chart 1

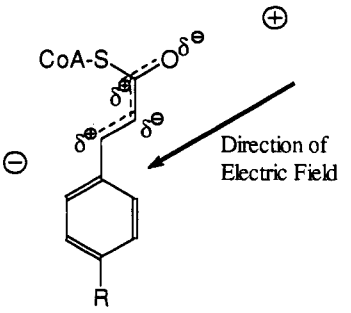

It must be kept in mind that the carbonyl in the free ligand is already solvated by water molecules, presumably through moderately strong H-bonds. We propose that the observed effects are caused by a strong electrophile at the C=O oxygen (this could be a positive charge or very strong hydrogen bonds) and a nucleophile near C-3 (a negatively charged group is the favored candidate), which generate a local electric field. This situation is illustrated in Chart 1. Such a model gives rise to a decrease in electron density on C-3, explaining the NMR results. It also, through the increased importance of resonance forms II and III, can explain the localized π electron polarization in the acryloyl group evidenced by the Raman data.

A similar push–pull model has been proposed for keto steroid isomerase to explain the polarization of the carbon–carbon double bond conjugated to the steroid carbonyl (Austin et al., 1992). In the keto steroid isomerase, the polarization is attributed largely to a tyrosine hydroxyl H-bond to the carbonyl and the ionized carboxylate of the general base responsible for proton abstraction. The results of Austin et al. show that the keto steroid isomerase enzyme also red shifts the conjugated carbon–carbon double bond more than can be explained by H-bond interactions with the carbonyl. However, the vibrational analysis of this system cannot be applied to crotonase since we have not identified an isolated carbonyl vibration in the Cin-CoA Raman spectra. Also, unlike the keto steroid isomerase, the electron polarization serves to enhance the electrophilicity at C-3 and consequently stabilizes the transition state for forming (and breaking) the C–O bond at the β carbon. This is an additional mechanistic role affected by polarization of the CoA thiol ester beyond simply enhancing the acidity of the α protons.

ACKNOWLEDGMENT

We acknowledge the assistance of Michael Ketterer of John Carroll University (University Heights, OH) in obtaining the ICP-MS metal analyses.

SUPPLEMENTARY MATERIAL AVAILABLE

Data for the spectroscopic characterization of CoA thiol esters (3 pages). Ordering information is given on any current masthead page.

REFERENCES

Allerhand, A. (1979) *Methods Enzymol. 61*, 458–549 (and references therein).

Austin, J. C., Kuliopoulos, A., Mildvan, A. S., & Spiro, T. G. (1992) *Protein Sci. 1*, 259–270.

Bahnson, B. J. (1990) Ph.D. Dissertation, Brown University, Providence, RI.

Bahnson, B. J., & Anderson, V. E. (1989) *Biochemistry 28*, 4173–4181.

Bahnson, B. J., & Anderson, V. E. (1991) *Biochemistry 30*, 5894–5906.
Brown, H. C., & Okamoto, Y. (1958) *J. Am. Chem. Soc. 80*, 4979.
Burke, J. R., & Frey, P. A. (1993) *Biochemistry 32*, 13220–13230.
Dahl, K. H., & Dunn M. F. (1984) *Biochemistry 23*, 4094–4100.
Dawson, R. M., Elliot, D. C., Elliot, W. H., & Jones, K. M., Eds. (1986) *Data for Biochemical Research, 3rd ed.*, Clarendon Press, Oxford, UK.
Dunn, M. F., & Buckley, P. D. (1985) in *Enzymology of Carbonyl Metabolism 2: Aldehyde Dehydrogenase, and Aldo/Keto Reductase and Alcohol Dehydrogenase*, pp 15–27, Alan R. Liss Publishers, New York.
Eliel, E. L. (1962) in *Sterochemistry of Carbon Compounds*, pp 330–334, McGraw-Hill, New York.
Ellman, G. L. (1959) *Arch. Biochem. Biophys. 82*, 70–77.
Fersht, A. (1985) in *Enzyme Structure and Mechanism*, 2nd ed., Wiley, New York.
Gerlt, J. A., & Gassman, P. G. (1992) *J. Am. Chem. Soc. 114*, 5928–5934.
Gerlt, J. A., Kozarich, J. W., Kenyon, G. L., & Gassman, P. G. (1991) *J. Am. Chem. Soc. 113*, 9667–9669.
Harada, I., & Takeuchi, H. (1986) in *Infrared and Raman Spectroscopy: Spectroscopy of Biological Molecules* (Clark, R. J. H., & Hester, R. E., Eds.) Vol. 13, pp 113–175, Wiley, New York.
Hass, G. M., & Hill, R. L. (1969) *J. Biol. Chem. 244*, 6080–6086.
Hassner, A., & Alexanian, V. (1978) *Tetrahedron Lett. 46*, 4478.
Jaffe, E., & Markham, G. D. (1987) *Biochemistry 26*, 4258–4264.
Kawaguchi, A., Yoshimura, T., & Okuda, S. (1981) *J. Biochem. 89*, 337–339.
Kim, M., Owen, H., & Carey, P. R. (1993) *Appl. Spectrosc. 47*, 1780–1783.
Knoop, F. (1905) *Beitr. Chem. Physiol. Pathol. 6*, 150–162.
Kuliopulos, A., Mildvan, A. S., Shortle, D., & Talalay, P. (1989) *Biochemistry 28*, 149–159.
Lefler, J. E., & Grunwald, E. (1963) in *Rates and Equilibria of Organic Reactions*, Wiley, New York.
Mao, L.-F., Chu, C., & Schulz, H. (1994) *Biochemistry 33*, 3320–3326.
Meyers, A. I., Spohn, R. F., & Linderman, J. F. (1985) *J. Org. Chem. 50*, 3633–3635.
Person, N. B. (1981) Ph.D. Dissertation, State University of New York at Buffalo.
Sarma, R. H., & Lee, C. H. (1975) *J. Am. Chem. Soc. 97* (5), 1225–1233.
Speisecke, H., & Schneider, W. G. (1961) *Tetrahedron Lett.* 468.
Steinman, H. M., & Hill, R. L. (1973) *J. Biol. Chem. 248* (3), 892–900.
Steinman, H. M., & Hill, R. L. (1975) *Methods Enzymol. 35*, 136–151.
Tsien, R. Y., Pozzan, T., & Rink, T. J. (1982) *J. Cell Biol. 94*, 325–394.
Varsanyi, G. (1969) in *Vibrational Spectra of Benzene Derivatives*, Academic Press, New York.
Waterson, R. M., & Hill, R. L. (1972) *J. Biol. Chem. 247*, 5258–5265.
Willadsen, P., & Eggerer, H. (1975) *Eur. J. Biochem. 54*, 247–252.
Yang, S. Y., Cuebas, D., & Schulz, H. (1986) *J. Biol. Chem. 261*, 15390–15395.